Gor Hakobyan and Bin Yang

High-Performance Automotive Radar

A review of signal processing algorithms and modulation schemes

©ISTOCKPHOTO.COM/TALAJ

The ongoing automation of driving functions in cars results in the evolution of advanced driver assistance systems (ADAS) into ones capable of highly automated driving, which will in turn progress into fully autonomous, self-driving cars. To work properly, these functions first must be able to perceive the car's surroundings by such means as radar, lidar, camera, and ultrasound sensors. As the complexity of such systems increases along with the level of automation, the demands on environment sensors, including radar, grow as well. For radar performance to meet the requirements of self-driving cars, straightforward scaling of the radar parameters is not sufficient. To refine radar capabilities to meet more stringent requirements, fundamentally different approaches may be required, including the use of more sophisticated signal processing algorithms as well as alternative radar waveforms and modulation schemes. In addition, since radar is an active sensor (i.e., it operates by transmitting signals and evaluating their reflections) interference becomes a crucial issue as the number of automotive radar sensors increases. This article gives an overview of the challenges that arise for automotive radar from its development as a sensor for ADAS to a core component of self-driving cars. It summarizes the relevant research and discusses the following topics related to high-performance automotive radar systems: 1) shortcomings of the classical signal processing algorithms due to underlying fundamental assumptions and a signal processing framework that overcomes these limitations, 2) use of digital modulations for automotive radar, and 3) interference-mitigation methods that enable multiple radar sensors to coexist in conditions of increasing market penetration. The overview presented in this article shows that new paradigms arise as automotive radar transitions into a more powerful vehicular sensor, which provides a fertile research ground for further investigation.

Introduction

When the idea of radar was first explored back in the late-19th and early-20th centuries, it was primarily seen as a technology for military applications. Other applications gradually emerged, however, and in the last four decades, radar has been studied for

Digital Object Identifier 10.1109/MSP.2019.2911722
Date of publication: 9 September 2019

 1053-5888/19©2019IEEE

use in the automotive sector for such applications as predictive crash sensing, obstacle detection, and braking [1]. The term *radar* is short for *radio detection and ranging*, an indication that radar is used to detect objects (obstacles and other road users) near the vehicle and to estimate their range as well as velocity and angle relative to the radar. For many years, production cars have made use of these capabilities to facilitate various driver-assistance functions, such as emergency brake assist and adaptive cruise control. More complex functions, such as fully autonomous driving, also rely heavily on radar as an environmental sensor [2], as it is capable of direct range and velocity measurements, can sense long distances ahead, is robust to bad weather and poor light conditions, and can be hidden behind a bumper.

A detailed overview of the status of automotive radar during its first several years is presented in [1]. The evolution of automotive radar is discussed in [3]. Other review articles provide overviews of the signal processing architecture and of the millimeter-wave technology for automotive radar [4], [5]. A more recent review article discusses the state-of-the-art signal processing algorithms for automotive radar and gives a bird's-eye view of estimation techniques, radar waveforms, and higher-level processing steps, such as tracking and classification [6].

This article gives an overview of the signal processing and modulation aspects of high-end automotive radar systems and discusses recent advances in these fields. We address the use of digital modulations, such as orthogonal frequency-division multiplexing (OFDM) and phase modulated continuous wave (PMCW) waveforms, for automotive radar and multiple-input, multiple-output (MIMO) radar in particular; discuss their potential benefits and challenges due to increased complexity; and survey recent research in this area. We also point out that classical automotive radar signal processing does not fully accommodate performance improvement through simple upscaling of the radar parameters (e.g., bandwidth, measurement time, antenna aperture) due to underlying fundamental assumptions. We provide a signal processing framework based on a more advanced signal model that surpasses these limits at a feasible computational cost. Next we explore the reliable operation of future automotive radar systems for which interference mitigation is vital and complete the discussion with a survey of interference-mitigation methods. These include some promising paradigms, such as interference-aware cognitive radar [7] and centralized coordination for interference avoidance [8].

Conventional automotive radar

Today, conventional automotive radar operates with a sequence of frequency-modulated continuous wave (FMCW) signals and is a well-studied research field [6], [9]. These systems transmit a series of analog-generated chirps, which are reflected and then mixed with the transmit (Tx) chirp at the receiver, resulting in a frequency proportional to the target distance and called *beat frequency*. The range processing is based on Fourier transform of the beat frequencies, and the Doppler-induced phase progression over the consecutive chirps is used for velocity estimation. Chirps are commonly designed to be short enough so that the distance-induced component of the beat frequency predominates, and their Doppler shift, i.e., the velocity component, is negligible (hence the name *fast chirp*). Figure 1(a) illustrates a sequence of identical FMCW chirps, the delayed and Doppler-shifted reflections of which after mixing with the Tx signal result in 2D complex exponentials in the baseband. A subsequent 2D Fourier transform yields the distance–velocity radar image. To localize targets in space, target angles are measured based on direction of arrival (DOA) of reflected signals with array processing techniques, most commonly via digital beamforming. Figure 1(b) shows the DOA-induced phase differences at receive (Rx) channels and the principle of digital beamforming that combines Rx signals with phases that digitally direct the beam to a certain DOA. In the simplest case, all three frequency-estimation tasks are solved jointly by a 3D Fourier transform, followed by power detection [10], parameter estimation, clustering and association of reflexes [11], object classification and tracking [12], data fusion [13], and other calculations.

Typical frequency bands for automotive radar are 24 and 77 GHz, with most of the manufacturers shifting toward 77 GHz for newer radar generations. This is due to larger available bandwidth (76–77 GHz for long-range and 77–81 GHz for short-range applications), higher Doppler sensitivity (and thus higher velocity resolution), and smaller antennas.

Automotive radar performance is measured according to the following main parameters: 1) resolution (ability to separate two closely spaced targets), 2) unambiguously measurable range (the range of parameter values that are unambiguously distinguishable), and 3) dynamic range (power ratio between the strongest and the weakest of detectable targets) in its measurement dimensions, i.e., distance, velocity, azimuth, and elevation angle.

For conventional Fourier-based signal processing, the radar resolution and unambiguous range for all of the aforementioned measurement parameters are directly determined by the sampling frequency and observation length in the corresponding dimension. For distance, the observation length is given by the bandwidth B, and its inverse determines the resolution with which the round-trip delays $\tau = 2d/c_0$ are measured, with d being the target distance and c_0 being the speed of light. Thus, the distance resolution is given by the following bandwidth: $\Delta d = c_0/(2B)$. Analogously, in the velocity dimension the Doppler resolution Δf_{D} is determined by the inverse of the measurement cycle duration T_{cycle}, i.e., $\Delta f_{\mathrm{D}} = 1/T_{\mathrm{cycle}}$. With $\Delta f_{\mathrm{D}} = 2\Delta v f_{\mathrm{c}}/c_0$, the velocity resolution is $\Delta v = c_0/(2 f_{\mathrm{c}} T_{\mathrm{cycle}})$. For DOA-induced spatial frequencies, the resolution can be derived analogously from the dimensions of the antenna array [14]. The previous discussion makes apparent that regardless of the radar waveform, a large bandwidth and a long measurement time are required for a high distance and velocity resolution.

To obtain a resolution higher than that of the conventional Fourier processing, superresolution frequency estimation methods can be applied in different radar measurement dimensions. Such methods can be coarsely classified into subspace-based, maximum-likelihood, or compressed-sensing methods. A review of high-resolution methods for array processing and for multidimensional automotive radar processing can be found in [14] and [15], respectively. An overview of compressed-sensing applications for radar is given in [16].

Digital radar

In parallel to the described fast-chirp radar, alternative automotive radar concepts based on digital modulations, such as OFDM [17] and PMCW [18], have been studied over the past few years. These concepts differ from FMCW radar in terms of generating waveforms digitally and performing demodulation in the digital domain. Broadly speaking, this is equivalent to operating with arbitrary digitally generated waveforms and matched filter-based processing at the receiver. For OFDM radar, this large degree of flexibility in the waveform choice enables communication and radar capabilities to be combined by embedding communication information into the radar waveform [17]. It further enables fully adaptive, software-defined behavior based on digitally generated waveforms. While more challenging in terms of practical realization—mainly due to analog-to-digital converters (ADCs) and significantly larger data loads—this opens up new dimensions for radar development and enables advanced radar concepts.

OFDM radar

The OFDM waveform is composed of a set of orthogonal complex exponentials [subcarriers; see the left-hand side of Figure 2(a)], the complex amplitudes of which are modulated with communication data or radar modulation symbols. The orthogonality of subcarriers results from the constraint of all subcarriers having a whole number of periods during one evaluation interval, called an *OFDM symbol* [see the right-hand side of Figure 2(a)]. As the discrete Fourier transform (DFT) exhibits the same characteristics, OFDM waveforms can be efficiently generated via inverse fast Fourier transform (IFFT) of the modulation symbols, i.e., complex amplitudes of OFDM subcarriers. Conversely, the communication data or radar modulation symbols can be efficiently extracted (demodulated) at the receiver based on FFT. From the communication standpoint,

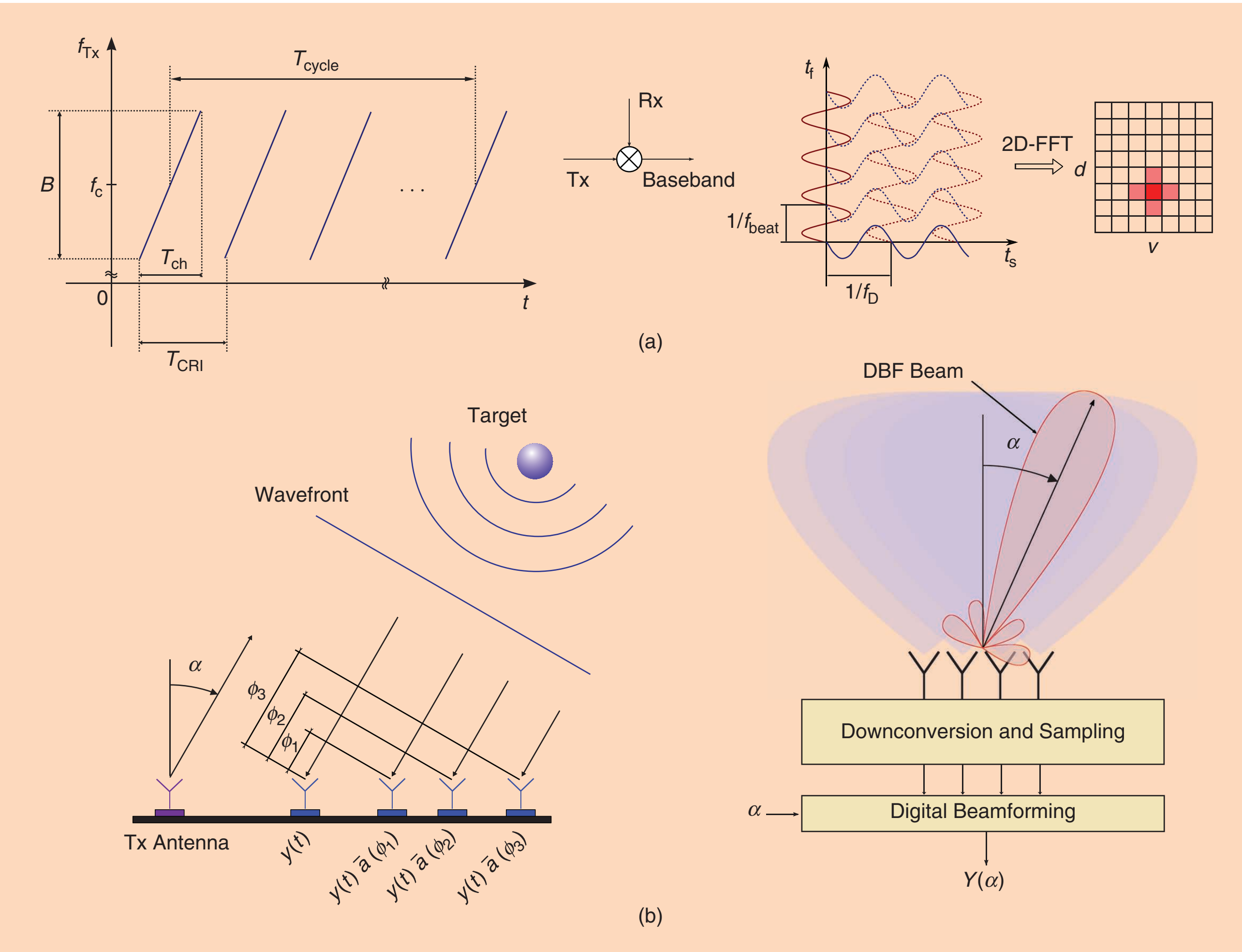

FIGURE 1. Graphs and illustrations showing the principle of distance, velocity, and DOA estimation for conventional fast-chirp automotive radar. (a) A sequence of identical FMCW chirps. The delayed and Doppler-shifted reflections of such chirps, after mixing with the Tx signal, result in 2D complex exponentials in the baseband. (b) The DOA-induced phase differences at Rx channels and the principle of digital beamforming that combines Rx signals with phases that digitally direct the beam to a certain DOA. B: bandwidth; f_c: carrier frequency; T_{CRI}: chirp repetition interval; T_{ch}: chirp duration; f_{beat}: beat frequency; f_D: Doppler shift; t_s: slow-time; d: distance; v: velocity; α: target angle; $y(\phi_n)$ received signal with a phase shift ϕ_n at the nth Rx antenna.

this achieves high spectral efficiency as well as simple extraction of communication data. Meanwhile, from the radar standpoint, it enables efficient digital demodulation of the radar waveform. OFDM not only enables favorable modulation for both applications, but it also combines both functionalities via a single waveform. This initially motivated research on OFDM radar. Currently, OFDM is often studied as a means for efficient implementation of digital, software-defined radar—independent of the communication aspect.

To prevent interference between consecutive OFDM symbols in a multipath channel, a cyclic prefix (CP) that contains repetition of the end portion of OFDM symbol is transmitted before the symbol [see the right-hand side of Figure 2(a)]. This converts the linear convolutive channel into a cyclic one, and thus time-of-flight delays result in cyclic shifts of OFDM symbols at the receiver. The block diagram in Figure 2(b) depicts the structure of the OFDM system. The OFDM symbols generated via IFFT are shifted into the radio-frequency (RF) band via a quadrature modulation and transmitted over the channel. From the perspective of radar, the channel represents objects in the vehicle's surroundings, i.e., the driving environment. At the receiver, the CP is removed from the quadrature demodulated signal, and the complex modulation symbols are obtained via an FFT. For OFDM radar signal processing illustrated in Figure 2(c), the subcarrier values of consecutive OFDM symbols are placed into a 2D measurement matrix. The radar waveform is demodulated based on spectral division, which cancels out the transmitted complex modulation symbols by elementwise

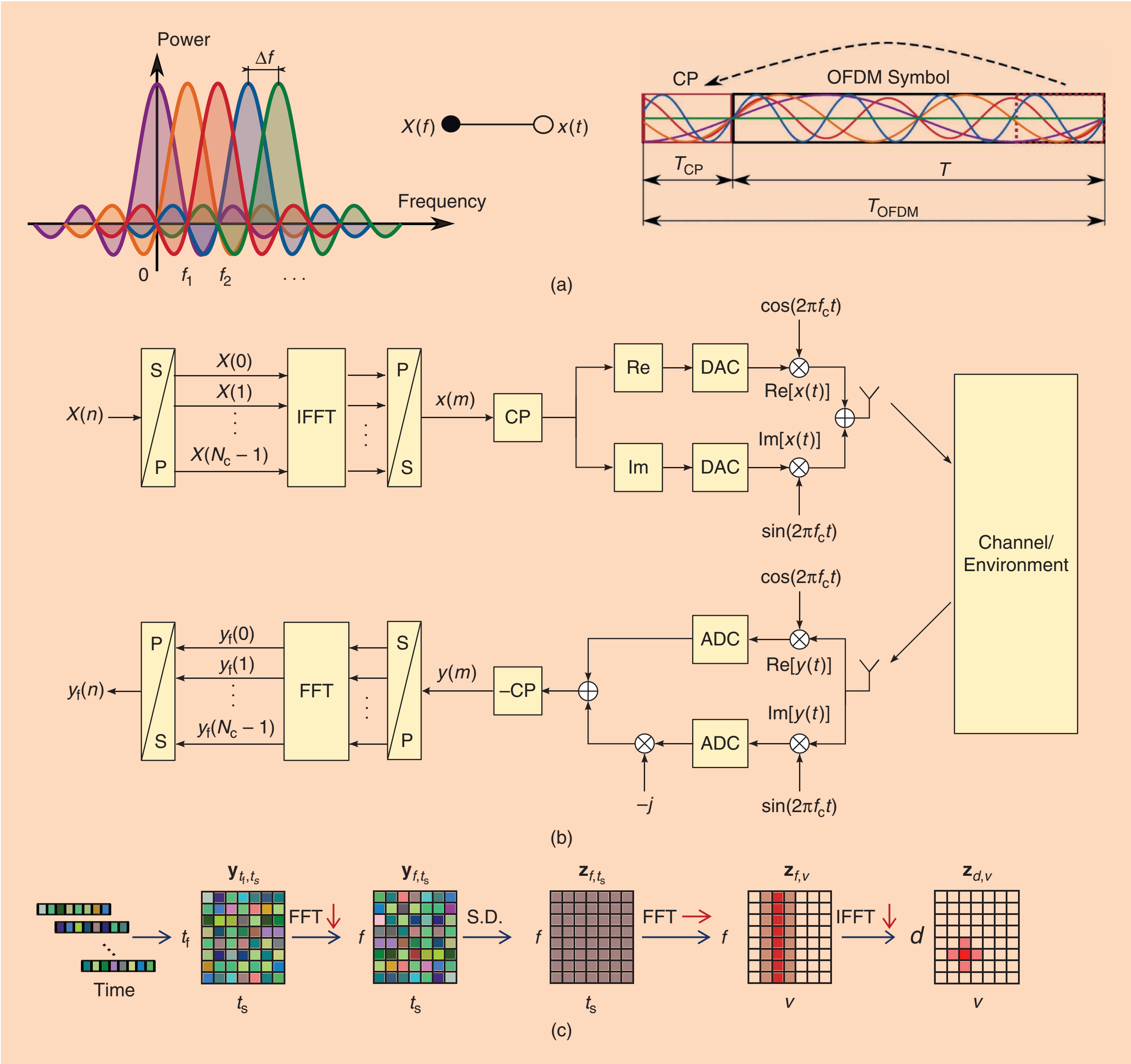

FIGURE 2. Illustrations showing the OFDM radar principle. (a) On the left, the OFDM spectrum and its inverse Fourier transform resulting in a time-domain OFDM symbol on the right. (b) The block diagram of the OFDM system. (c) The signal processing steps of OFDM radar. S.D.: spectral division; Re, real, Im, imaginary; P/S, the parallel-to-serial blocks; S/P, the serial-to-parallel blocks.

multiplication with their inverse values (conjugate in case of unitary subcarrier amplitudes). This operation reduces the measurement matrix to a sum of 2D complex exponentials, the frequencies of which over the OFDM subcarriers and symbols correspond to the distances and velocities of the radar targets. Similar to fast-chirp radar, a 2D-FFT processing (IFFT over subcarriers, FFT over symbols) leads to the distance–velocity radar image.

We make the following observations regarding the OFDM radar signal processing.

- For unitary subcarrier amplitudes, the distance processing is equivalent to matched filtering implemented efficiently in the frequency domain.
- The described signal processing neglects the Doppler shift of OFDM subcarriers, which might lead to intercarrier interference (ICI). To limit ICI to a negligible level, the subcarrier spacing Δf must be much larger than the maximum possible Doppler shift $f_{\mathrm{D,max}}$, e.g., $\Delta f = 10 f_{\mathrm{D,max}}$ [17]. This limits, however, the parametrization freedom, especially for long-range and highly dynamic applications, such as front long-range automotive radar.
- Under conditions of unitary subcarrier amplitudes and negligible Doppler shift, the waveform has no influence on the signal processing performance. Thus, it can carry communication data or be optimized with respect to peak-to-average power ratio for radar (e.g., [19]).
- The distance and velocity processing is done in two independent dimensions and no coupling between them is considered. Since the target velocity in practice affects both measurement dimensions, this can be interpreted as simplification of the 2D matched filtering into two separate one-dimensional matched filters, one per each measurement dimension. Analogous to fast-chirp radar, this ignores the range change for moving targets, and thus assumes all OFDM symbols to have the same delay.

Since OFDM radar demodulates the radar waveform in the digital domain, the entire signal bandwidth needs to be sampled, contrary to fast-chirp radar that samples only the bandwidth of beat frequencies. This makes the practical realization of OFDM radar more challenging, imposing high demands on ADCs, memory, and digital signal processing. Some of the ongoing research in [7] and [20]–[22] focuses on methods for limiting the instantaneous bandwidth, and thus the sampling rates. Whereas [20] covers a larger bandwidth by sweeping in multiple steps (called *stepped OFDM*), [7] and [21] combine OFDM waveform with a chirp to increase the effective bandwidth. By randomly occupying smaller portions of the full bandwidth at each time instance, [22] aims to reduce the sampling rates of OFDM radar with a compressed-sensing approach.

PMCW radar

An alternative implementation of digital radar uses a sequence of waveforms generated by phase modulation of continuous waves [18]. The waveform generation via biphase modulation of the RF-carrier signal with 0° and 180° phase shifts is particularly simple to implement in CMOS technology [18]. At the receiver, a bank of digitally implemented correlators is used for range processing. The Doppler processing is done via an FFT over a sequence of consecutive coded waveforms, analogous to fast-chirp or OFDM radars. The block diagram of a PMCW radar is shown in Figure 3. For favorable autocorrelation properties and thus high dynamic range in range estimation, the selection of a proper code sequence is essential. Using orthogonal codes, multiple Tx channels can operate simultaneously based on code-domain separation, allowing MIMO processing. Furthermore, a meaningful code selection can provide favorable properties in terms of robustness against interference. As for OFDM radar, Doppler shift has an adverse effect on PMCW waveforms in terms of auto- and cross-correlation properties, and needs to be accounted for by parametrization, code choice, or compensation in signal processing.

Discussion of modulation schemes

Fast-chirp, OFDM, and PMCW radars share the same principle of distance–velocity measurement: time-of-flight-based coherent distance estimation via pulse compression (fast-time) and Doppler-based velocity estimation via FFT over a series of consecutive waveforms (slow-time). For all three systems, the resolution and unambiguous range depend solely on observation length (i.e., bandwidth in fast-time and measurement time in slow-time) and sampling rate (ADC rate in fast-time and waveform repetition rate in slow-time). In terms of hardware effort, fast-chirp radar has an advantage due to analog mixing, i.e.,

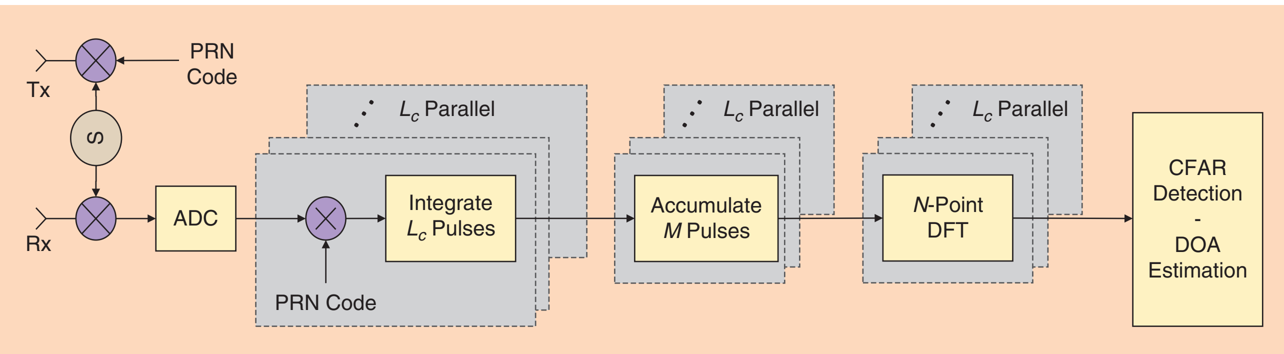

FIGURE 3. A schematic view of PMCW radar. The carrier signal is modulated with a pseudorandom noise (PRN) code. The distance processing is based on L_c digital correlators, followed by DFT-based Doppler processing [18]. CFAR: constant false alarm rate.

demodulation, resulting in significantly reduced sampling rates for beat frequencies. In contrast, digital radar requires sampling of the entire bandwidth, i.e., higher ADC rates, memory, and computational demands. The software-defined capabilities of such radar allow, however, a substantially larger flexibility in operation. As automotive radars become increasingly complex, digital radar with software-defined modulation allows more features with respect to adaptive and multifunction behavior, advantageous MIMO concepts, and robustness against interference based on large waveform diversity.

MIMO radar

The use of MIMO radar techniques is a well-established approach for improved angle estimation with radar [23]. MIMO radar uses multiple channels at both the Tx and the Rx sides such that the number of paths between the radar and the target is efficiently increased. That is, with the number of paths being the product of the number of Tx and Rx channels, MIMO radar obtains more paths than the number of physical channels. These paths can be arranged into a larger virtual aperture with more elements, as depicted in Figure 4, and thus improve the angular resolution and estimation accuracy of the radar. The resulting virtual aperture can then be processed with conventional array processing techniques. The main challenge for MIMO radar is thus the choice of waveforms such that the signals from different Tx antennas can be clearly distinguished, i.e., the multiplexing of the Tx channels. For high-performance automotive radar, efficient multiplexing of a large Tx array is a key factor for achieving a high angular resolution in both azimuth and elevation. Conventionally, Tx antennas are multiplexed in time [24], frequency [25], or code [26].

Because of its simplicity, time-division multiplexing (TDM) with equidistantly interleaved chirps is the most common multiplexing technique for fast-chirp radar. However, this approach allows only one antenna to be active at a time, and thus limits considerably the number of Tx antennas that can be multiplexed. Some more advanced multiplexing methods for fast-chirp radar include the following [6]:

- *Beat frequency multiplexing*: Chirps of multiple Tx channels run parallel with an offset in time and/or frequency, such that the beat frequencies of different Tx channels appear as frequency division multiplexed (FDM). Let us denote the base chirp $x_0 = \exp(j\pi K t^2)$ with K being the chirp slope. For chirps with frequency offset, the signal of the nth Tx channel is $x_n = \exp(j\pi[Kt^2 + 2n\Delta f_{Tx} t])$, the offset Δf_{Tx} being larger than the maximum beat frequency $f_{\text{beat,max}}$. Analogously, for chirps offset in time, the signal of the nth Tx channel is $x_n = \exp(j2\pi K[t - n\Delta\tau_{Tx}]^2)$, with $\Delta\tau_{Tx}$ being larger than the maximum round-trip delay $\tau_{\max}$. This allows tighter spacing of chirps than conventional TDM or FDM, e.g., more efficient use of time–frequency resources.
- *Slope diversity multiplexing*: Multiple Tx channels transmit chirps of the same bandwidth but different duration, i.e., slope. The signal of the nth Tx antenna is then $x_n = \exp(j\pi[K + \Delta K_n]t^2)$, with ΔK_n being the slope difference to the base chirp slope K. At the receiver, the radar signal is demodulated with multiple slopes, each of the signals resulting in beat frequency for the corresponding Tx channel and chirp for other channels. The subsequent FFT processing focuses the signals with constant beat frequency and spreads the remaining chirp signals. This achieves a separation between Tx channels, albeit in a nonorthogonal manner and thus with limited dynamic range.
- *Slow-time phase modulation based multiplexing*: The phase of each chirp (or any waveform in general) in slow-time is modulated to multiplex Tx channels. That is, for the nth Tx antenna, the phase over slow-time is modulated with $\exp(j2\pi C_n(t_s))$. When modulated with a complex exponential (linear phase progression $C_n(t_s) = f_s t_s$), this leads to a Doppler offset between the Tx channels. This is advantageous in applications where the maximum possible Doppler shift is smaller than the unambiguously measurable Doppler range (e.g., at lower carrier frequencies). Alternatively, slow-time phases can be modulated with orthogonal codes to multiplex Tx channels. This requires Doppler-robust codes, which typically exhibit limited dynamic range in the velocity estimation.

Due to its multicarrier structure, OFDM radar allows even more freedom with respect to multiplexing for MIMO radar. OFDM subcarriers can be individually assigned to a Tx antenna, which enables the generation of various orthogonal waveforms for MIMO radar. With this approach, Tx antennas can operate simultaneously using the entire bandwidth. OFDM-specific multiplexing methods include the following:

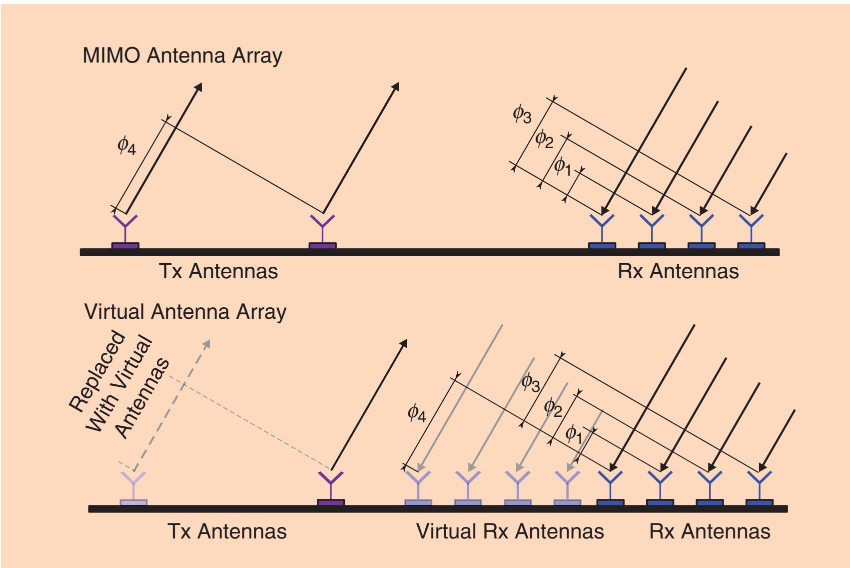

FIGURE 4. A diagram showing the principle of MIMO radar and virtual apertures.

- *Equidistant subcarrier interleaving* [17]: Subcarriers of OFDM radar are interleaved equidistantly over multiple Tx antennas (every N_{Tx}th subcarrier is assigned to one of the N_{Tx} Tx antennas), such that all Tx channels use the entire bandwidth simultaneously. While maintaining the distance resolution, this reduces the unambiguously measurable distance range, as the spacing between subcarriers transmitted from one Tx antenna increases from Δf to $N_{\mathrm{Tx}}\Delta f$ (i.e., the sampling rate of distance-induced complex exponentials decreases). This method is thus less suitable for long-range applications.
- *Nonequidistant subcarrier interleaving* [27]: To overcome the drawback of equidistant subcarrier interleaving in terms of reduced unambiguously measurable distance range, the OFDM subcarriers can be interleaved nonequidistantly. This implies a nonuniform sampling of distance-induced complex exponentials that maintains unambiguous distance range for each Tx channel. Since for nonuniform sampling, FFT-based processing leads to increased sidelobes, nonequidistant subcarrier interleaving requires more complex distance processing, e.g., based on compressed sensing. The nonequidistant subcarrier interleaving can be kept the same in slow-time (same for all OFDM symbols), or changed dynamically for each OFDM symbol, resulting in 2D nonuniform sampling patterns [28].
- *Space–time block codes* [19]: To simultaneously use all subcarriers by all Tx antennas, OFDM subcarriers can be modulated with space–time block codes. This makes it possible to maintain distance estimation parameters for each channel. It reduces, however, the unambiguous velocity range, as consecutive OFDM symbols constituting a block of code are required for distance processing.

For PMCW radar, multiple Tx channels can be multiplexed based on orthogonal codes—in both fast- and slow-times [18]. To this end, the low cross correlation of codes (also under the condition of Doppler shift) is essential for effective separation of MIMO channels.

Evidently, both fast-chirp and digital radars enable advanced modulation-specific multiplexing schemes. As multiplexing implies sharing of available resources (e.g., time, frequency) between multiple channels, each multiplexing method leads to some specific drawbacks compared to a single Tx channel in terms of distance–velocity estimation. By a proper choice of the multiplexing method, these drawbacks are minimized, while obtaining improved DOA processing based on MIMO radar.

A further important aspect of MIMO radar to consider when choosing a multiplexing method is the coherency between the Tx channels. Maximum coherency is obtained when all Tx channels transmit simultaneously using the same bandwidth. In case of a time offset between the measurements of Tx channels, the target motion leads to Doppler-induced phase shifts between channels that add up to the DOA-induced phase progression. Analogously, different carrier frequencies of Tx channels imply a range-dependent, unknown phase shift $\exp(j2\pi\Delta f_{\mathrm{c,Tx}}2d/c_0)$ adding to the DOA-induced phase differences, with $\Delta f_{\mathrm{c,Tx}}$ denoting the carrier frequency offset of a Tx channel from a reference frequency f_{c}. In case one of these phase components becomes dominant (e.g., for FDM with very large frequency offsets), the MIMO-based DOA processing becomes impractical. The coherency aspect of MIMO processing favors subcarrier interleaving schemes of OFDM radar, as they enable simultaneous transmission from all Tx channels with identical or very close carrier frequencies.

Limits of conventional range-Doppler processing

For both fast-chirp and digital radars, the conventional automotive radar signal processing assumes that problems estimating the range (distance), velocity, and angle can be solved by processing the following three independent measurement dimensions (ignoring elevation for simplicity of discussion): 1) fast-time (single chirp, OFDM, or PMCW symbols), 2) slow-time (consecutive waveforms), and 3) spatial domain (array elements). These measurement dimensions are, however, not entirely independent. For range-Doppler processing in particular, the range of the moving target changes over consecutive waveforms, and may thus lead to a migration of the target peak between range cells over slow-time, i.e., range migration [7], [29].

Similarly, the Doppler processing of the conventional automotive radar is based on the narrowband assumption, as all frequencies in the signal are approximated by the carrier frequency. As Doppler effect is frequency dependent, each frequency in the signal undergoes a different Doppler shift for wideband systems, and thus yields a different velocity estimate. Analogous to range migration, this leads to a Doppler frequency migration. Both effects prevent the 2D Fourier transform from collecting the entire signal energy into a single range–velocity cell and thus reduce the resolution both in range and velocity [7].

Both the range and Doppler frequency migration originate from the motion of the target during the measurement. Range migration occurs when the range change during the measurement $d_{\mathrm{mig}} = vT_{\mathrm{cycle}}$ exceeds one range cell (resolution) $\Delta d = c_0/(2B)$, i.e., for a target with the following velocity:

$$|v| \geq \frac{c_0}{2BT_{\mathrm{cycle}}}. \tag{1}$$

Consequently, the range migration normalized to a range cell is the following:

$$\zeta_{\mathrm{RM}} = \frac{d_{\mathrm{mig}}}{\Delta d} = \frac{2vBT_{\mathrm{cycle}}}{c_0}. \tag{2}$$

From (2), the range migration is large for a large time–bandwidth product BT_{cycle} and scales with the target velocity. The same equation describes the amount of Doppler frequency migration [7], since both effects are inherently linked. In fact, they are representations of the same phenomenon in two different dimensions: range–slow-time and frequency–Doppler-estimate, respectively. Hence, for moving targets, range and Doppler frequency migration limit the simultaneously achievable range and velocity resolution, imposing an upper bound jointly on both parameters. For a typical bandwidth of 1 GHz and measurement time of 20 ms, one cell migration occurs for velocities $v > 7.5$ m/s. From the application perspective, the impact of migration effects is especially adverse during driving, as the stationary targets appear moving relative to radar and thus are affected by migration-induced smearing in the radar image.

A further problem especially relevant for digital modulations, such as OFDM or PMCW, is the Doppler shift of the signal frequencies. For OFDM radar, this leads to ICI between subcarriers [17], [30], and for coded waveforms their cross- and autocorrelation characteristics deteriorate. Whereas the classical approach accounts for Doppler shift by limiting the system parametrization such that the maximum Doppler shift is still acceptable, this becomes a critical limitation for high-performance automotive radar.

Signal processing framework for high-performance radar

As the discussion in the previous section indicates, a signal processing framework based on a more rigorous signal model is needed to fully gain the benefits from upscaling of radar parameters for increased estimation performance. This implies that the current 2D-FFT-based processing has to be replaced with a better approximation of a 2D-matched filter. An approach to achieve this for a single target (or multiple targets with the same velocity) was proposed in [31]. Next, we summarize the research in [7], [29], and [30] and present in general terms a signal processing framework capable of migration-free and Doppler-robust range–velocity processing at a feasible computational cost and for an arbitrary number of targets. We formulate it for arbitrary radar waveforms.

Consider an automotive radar transmitting a series of identical waveforms (e.g., FMCW chirps, OFDM, or PMCW symbols) for distance–velocity estimation:

$$x_{\mathrm{RF}}(t) = x(t - \mu T_{\mathrm{sym}})\exp(j2\pi f_{\mathrm{c}}[t - \mu T_{\mathrm{sym}}]), \tag{3}$$

where $x(t)$ is the waveform in $0 < t < T_{\mathrm{sym}}$ that repeats periodically over slow-time $t_s = \mu T_{\mathrm{sym}},\ \mu \in [0, N_{\mathrm{sym}} - 1]$, with N_{sym} being the number of waveforms (e.g., OFDM symbols) during one measurement cycle. Let us define the fast-time $t_{\mathrm{f}} = t - \mu T_{\mathrm{sym}}$.

Consider the radar signal in (3) reflected from a moving target at a time-dependent range

$$d(t) = d_0 + vt = d_0 + vt_{\mathrm{f}} + vt_{\mathrm{s}} \tag{4}$$

and let us denote the corresponding time-dependent round-trip delay: $\tau(t) = 2d(t)/c_0 = \tau_0 + \tau_{\mathrm{v}}(t_{\mathrm{f}}) + \tau_{\mathrm{v}}(t_{\mathrm{s}})$, where $\tau_0 = 2d_0/c_0$ and $\tau_v(t) = 2vt/c_0$.

After downconversion, the delayed signal at the receiver is as follows:

$$\begin{aligned} y(t) &= Ax_{\mathrm{RF}}(t - \tau(t))\exp(-j2\pi f_{\mathrm{c}} t_{\mathrm{f}}) \\ &= Ax(t_{\mathrm{f}} - \tau(t))\exp(-j2\pi f_{\mathrm{c}}\tau(t)), \end{aligned} \tag{5}$$

where A denotes the amplitude change of the signal through propagation and reflection. By representing $\tau(t)$ with its time-independent (τ_0), fast-time ($\tau_{\mathrm{v}}(t_{\mathrm{f}})$), and slow-time ($\tau_{\mathrm{v}}(t_{\mathrm{f}})$) components, we can examine the following six elements of the signal model in (5):

1) The waveform $x(t)$ is delayed by τ_0 due to the initial target distance d_0. This term is commonly used for range processing.
2) The additional delay in fast-time $\tau_{\mathrm{v}}(t_{\mathrm{f}})$ in the argument of x denotes the delay of each time sample of the waveform, i.e., represents the Doppler-induced stretching/compression of the signal. For typical automotive applications, this term is negligible [7].
3) The third delay component $\tau_{\mathrm{v}}(t_{\mathrm{s}})$ in the argument of x is the range change over slow-time due to the target's motion. When ignored, this term can cause range and Doppler frequency migration.
4) The first exponential term $\exp(-j2\pi f_{\mathrm{c}}\tau_0)$ in (5) represents a constant phase shift for all samples and is irrelevant for the range and velocity processing.
5) The terms $\exp(-j2\pi f_{\mathrm{c}}\tau_{\mathrm{v}}(t_{\mathrm{f}})) = \exp(j2\pi f_{\mathrm{D}} t_{\mathrm{f}})$ describes the Doppler shift $f_{\mathrm{D}} = -2vf_{\mathrm{c}}/c_0$ of the waveform in fast-time. It has an adverse effect on the range estimation (e.g., leads to ICI in case of OFDM radar) when not taken into account.
6) The last term $\exp(-j2\pi f_{\mathrm{c}}\tau_{\mathrm{v}}(t_{\mathrm{s}})) = \exp(j2\pi f_{\mathrm{D}} t_{\mathrm{s}})$ is the Doppler-induced phase progression over slow-time. It is commonly used for Doppler processing.

The conventional radar signal processing simplifies (5) to $Ax(t_{\mathrm{f}} - \tau_0)\exp(j2\pi f_{\mathrm{D}} t_{\mathrm{s}})$. Ignoring the third and fifth terms in (5), the range and velocity estimation problems can be decoupled to fast-time and slow-time dimensions, respectively. The first term is then used for the range processing in fast-time, and the remaining sixth term for Doppler processing is used in slow-time. For high-performance automotive radar, however, neither the third nor the fifth term in (5) can be ignored, as this would lead to migration effects and reduced performance in range processing. Later, we describe a signal processing framework based on a more-precise signal model. Table 1 gives an overview of how signal processing terms in (5) are treated by the conventional Fourier-based range-Doppler processing and by the reviewed framework (the terms in the argument of x are discussed individually).

Ignoring the second and fourth terms that are irrelevant, the signal model in (5) can be rewritten in the fast-time and slow-time dimensions as follows:

$$y(t_{\mathrm{f}}, t_{\mathrm{s}}) = Ax(t_{\mathrm{f}} - [\tau_0 + \tau_{\mathrm{v}}(t_{\mathrm{s}})])\exp(j2\pi f_{\mathrm{D}}[t_{\mathrm{f}} + t_{\mathrm{s}}]). \tag{6}$$

The Fourier transform of (6) in fast-time leads to the following:

$$y(f, t_{\mathrm{s}}) = AX(f - f_{\mathrm{D}})\exp(-j2\pi f[\tau_0 + \tau_{\mathrm{v}}(t_{\mathrm{s}})])\exp(j2\pi f_{\mathrm{D}} t_{\mathrm{s}}), \tag{7}$$

where $X(f - f_{\mathrm{D}})$ is the Doppler-shifted spectrum of the radar waveform, the second exponential term is the slow-time-dependent target distance, and the last term is the Doppler shift over slow-time. The representation in (7) makes apparent that the range migration is caused by the slow-time-dependent range change $\exp(-j2\pi f\tau_{\mathrm{v}}(t_{\mathrm{s}}))$. To demonstrate that the same term is responsible for the Doppler frequency migration, we rewrite (7) as follows:

$$y(f, t_{\mathrm{s}}) = AX(f - f_{\mathrm{D}})\exp(-j2\pi f\tau_0)\exp(j2\pi[f_{\mathrm{D}} + \hat{f}_{\mathrm{D}}(f)]t_{\mathrm{s}}), \tag{8}$$

where $\hat{f}_{\mathrm{D}} = -2vf/c_0$ is the Doppler frequency migration. The representation in (8) shows that the Doppler-induced complex

Table 1. Summary of terms in the signal model in (5).

Term	Referred To As	Conventional Processing	Reviewed Framework
$x(t-\tau_0)$	1) Delay	For range (distance) estimation	
$x(t-\tau_v(t_f))$	2) Doppler scaling (fast-time)	Neglected	
$x(t-\tau_v(t_s))$	3) Migration term	Neglected	Compensated by ACMC
$\exp(-j2\pi f_c\tau_0)$	4) Constant phase shift	Ignored (irrelevant)	
$\exp(j2\pi f_D t_f)$	5) Doppler shift (fast-time)	Neglected	Compensated by ACDC
$\exp(j2\pi f_D t_s)$	6) Doppler term	For velocity estimation	

exponentials over the slow-time are frequency dependent for $f \in [-B/2, B/2)$. By compensating this frequency dependency, both the range and Doppler frequency migration can be prevented, since a single term is causing both effects.

To accomplish this, we can start from the Doppler processing and perform it for each frequency in $f \in [-B/2, B/2)$ with a kernel that scales the frequency axis to match $(f_D + \hat{f}_D(f))$ as opposed to the conventional Fourier transform matching to f_D [7], [30]. This operation scales proportionally the Doppler grid for each frequency, such that each frequency yields the same Doppler estimate. This results in the following migration-free Doppler spectrum in slow-time:

$$\begin{aligned} y(f,\hat{v}) &= \sum_{\mu=0}^{N_{\mathrm{sym}}-1} y(f,t_s)\exp\left(-j2\pi[f_c+f]\frac{2\hat{v}}{c_0}\mu T\right) \\ &= AX(f-f_D)\exp(-j2\pi f\tau_0)\cdot D_{N_{\mathrm{sym}}}\left(\pi[f_c+f]\frac{2[v-\hat{v}]}{c_0}T\right), \end{aligned} \tag{9}$$

where $D_N(x) = \exp(j[N-1]x/2)\cdot\sin(Nx/2)/\sin(x/2)$ denotes the Dirichlet kernel and represents the Doppler spectrum of the target, with maximum at the velocity cell $\hat{v} = v$. This operation compresses the energy of each target into the corresponding Doppler cell that is same along the frequency dimension and thus migration-free. Subsequently, the Doppler shift of the waveform can be compensated next by a frequency shift of each velocity cell by its corresponding Doppler shift. This will implicitly correct the Doppler shift for the entire radar signal, as the energy of each target is now focused in the corresponding velocity cell. For the cell $\hat{v}$ corresponding to the target velocity v, the Dirichlet kernel in (9) becomes $D_{N_{\mathrm{sym}}}(0) = 1$. Transforming $y(f,\hat{v})$ back to the fast-time domain, we can correct the Doppler shift for the cell $\hat{v} = v$ by the following:

$$\begin{aligned} y(t_f,\hat{v}) &= Ax(t_f-\tau_0)\exp(j2\pi f_D t_f)\exp\left(j2\pi\frac{2\hat{v}}{c_0}f_c t_f\right) \\ &= Ax(t_f-\tau_0). \end{aligned} \tag{10}$$

The subsequent range processing can be conventionally performed based on a matched filter with knowledge of the waveform $x(t_f)$. This results in a range–velocity spectrum free of migration effects and Doppler-induced performance degradation.

The described idea of migration compensation through scaling of the velocity axis is the basis for the all-cell migration compensation (ACMC) for automotive radar in [7] as well as the Keystone transform in [29] for synthetic aperture radar. The linear scaling of the velocity axis can be efficiently implemented based on chirp-Z transform, which has an order of computational complexity $O(N\log N)$ that is the same as for FFT processing. The idea of Doppler shift compensation for all cells is known as all-cell Doppler correction (ACDC) [30]. The correction step is based on elementwise multiplication, and thus its computational cost is negligible (though it might need transforms between time and frequency domains, depending on implementation). This makes the described signal processing framework feasible for real-time automotive radar implementation as well as for other multitarget applications with a sequence of identical waveforms and negligible higher-order motion terms [see (4)]. The steps of the presented framework are depicted in Figure 5 and compared to the conventional radar processing on the example of OFDM radar.

Figure 6 shows measurement results of a car driving toward an OFDM-MIMO radar prototype [7]. In Figure 6(a), OFDM subcarriers undergo a Doppler shift 0.34 times the subcarrier spacing ($f_D/\Delta f = 0.34$) by reflecting from the moving car (see [30] for further details on the measurement setup). The conventional 2D-FFT processing without Doppler compensation thus results in a considerable level of ICI, constituting itself as a bright trace along the distance axis in the velocity cell of the target (Figure 6(a), left; around $v \approx -19$ m/s). In contrast, by shifting back the Doppler frequencies for each velocity cell, ACDC prevents Doppler-induced performance degradation for the entire radar image [30]. The target energy is focused into its distance–velocity cell ($d \approx 20$ m; $v \approx -19$ m/s), obtaining full signal-to-noise ratio gain and preventing dynamic range reduction. Further performance analysis on ACDC is available in [7] and [30].

To study the migration effects on a real-world example, Figure 6(b) presents a measurement with a bandwidth of 625 MHz and measurement time of 39.4 ms. According to (2), for the car moving with $v \approx -23$ m/s, conventional Fourier processing results in a range and Doppler frequency migration of more than three cells. Note that the scale of migration is equivalent to that of a system with a 1.25-GHz bandwidth and 19.7-ms measurement time, and thus is representative of automotive radar. With conventional Fourier processing, range migration leads to a smearing of the target peak of more than three cells over the range axis. The Doppler frequency migration results additionally in smearing of the same scale over the velocity axis. In Figure 6(b), left, this is particularly apparent for the corner reflector mounted on the roof of the vehicle to represent a distinct point target (smeared square around $d \approx 16$ m and $v \approx -23$ m/s). Figure 6(b), right, shows the same radar image when processed with ACMC. For the entire image, no migration-induced smearing of the peaks occurs. This is particularly clear for

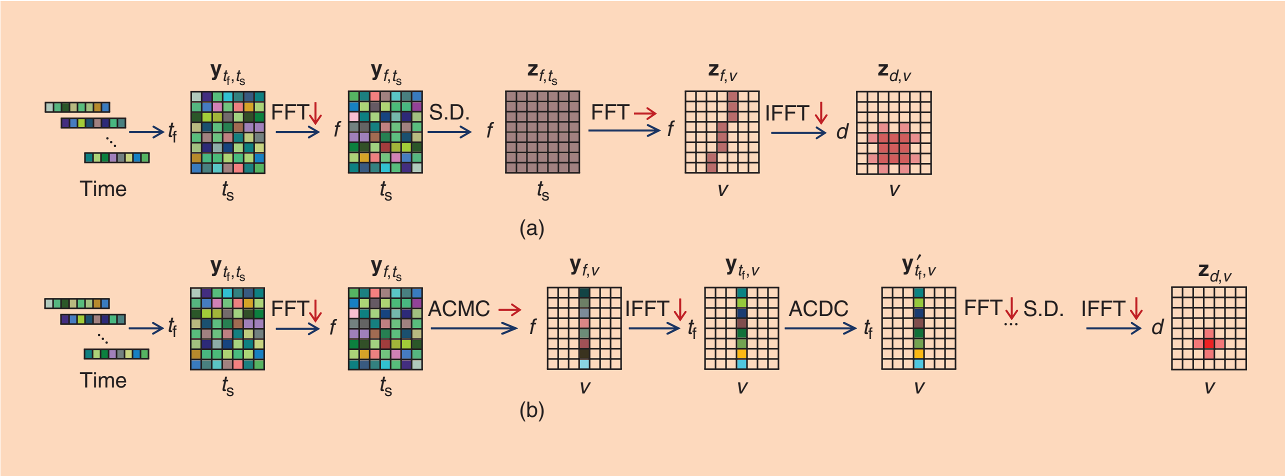

FIGURE 5. An illustration comparing conventional Fourier-based processing with the reviewed migration and ICI-free signal processing framework on the example of OFDM radar [7]. (a) 2D-FFT processing. (b) ACDC- and ACMC-based processing. S.D.: spectral division.

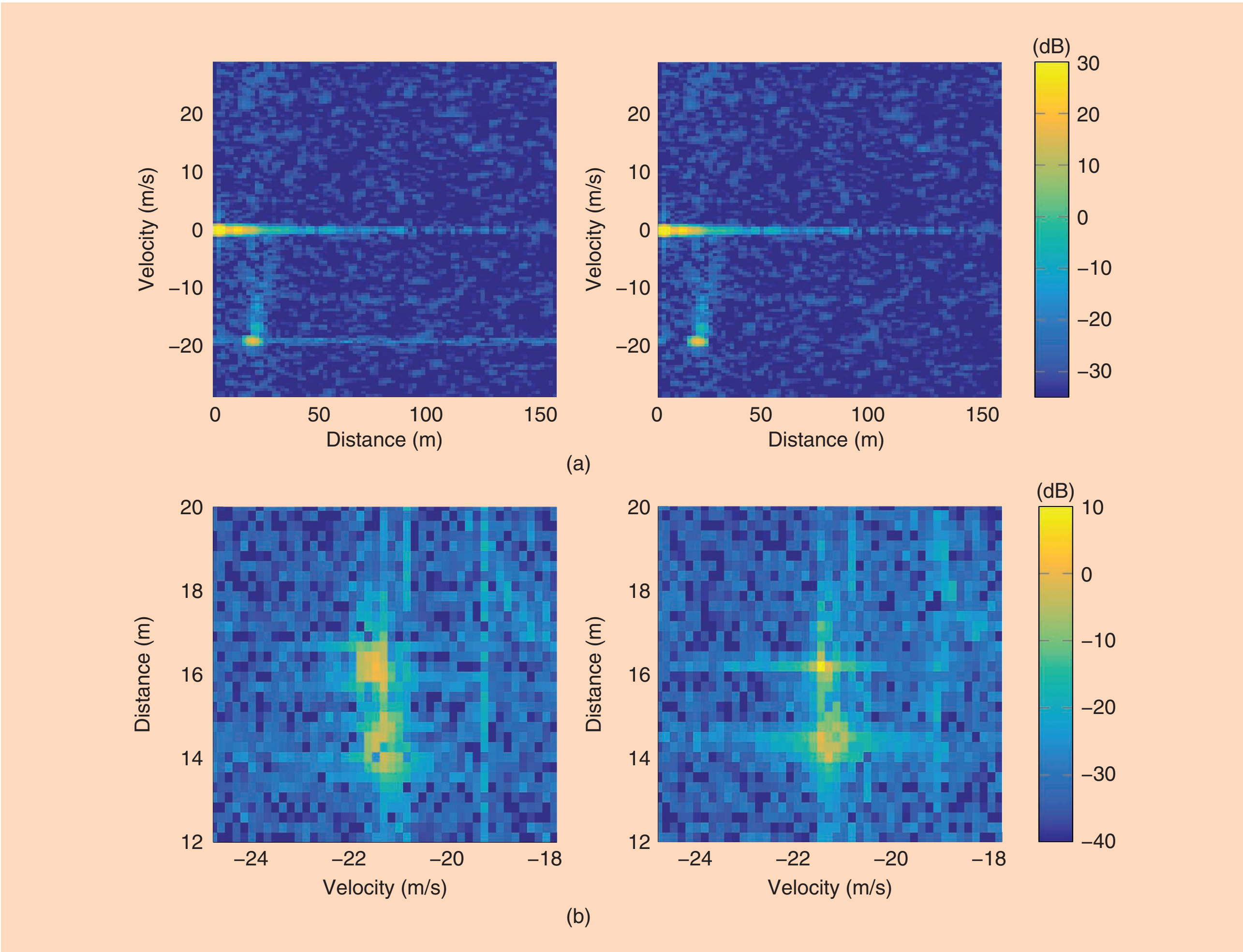

FIGURE 6. Radar images of an approaching car measured with an OFDM-MIMO radar prototype. The results for 2D-FFT processing make apparent the need for both Doppler-shift and target-motion compensation. The described migration and ICI-free processing overcomes limitations of 2D-FFT. (a) ACDC (right) versus conventional 2D-FFT (left) [30]. The bright trace along the distance axis from the moving car is induced by ICI, which does not occur for ACDC. (b) ACMC (right) versus conventional 2D-FFT (left) [7]. The moving car with a corner reflector mounted on top results in a range and Doppler frequency migration of around 3.5 cells. For 2D-FFT, target reflections are smeared due to range and Doppler-frequency migration, whereas ACMC collects the signal energy into a sharp peak.

the corner reflector, the energy of which is coherently focused into a sharp peak. This illustrates that ACMC prevents the migration-induced degradation of the range and velocity resolution inherent to the conventional 2D-FFT processing. For moving targets, this allows longer coherent integration times and a higher simultaneous range and velocity resolution. Further performance analyses of ACMC are available in [7].

Interference mitigation

As the number of automotive radar sensors on the road increases, robustness against interference becomes a more important challenge for reliable radar operation. Broadly speaking, high-end automotive radars are more susceptible to interference due to greater use of the time–frequency resources (e.g., large bandwidth, long measurement time). Considering the strict requirements on reliability of operation, interference mitigation becomes a core component of high-performance automotive radars. Generally, to avoid interference, signals of different radars must be separable at least in one dimension, e.g., time, frequency, space, or code/waveform [32]. The main methods for radar interference mitigation can be clustered into the following categories.

- *Detect and suppress at the receiver*: Interference is detected from the measurement data and suppressed via dropping the affected data and reconstructing their values (see [33] and [34] for FMCW radar and [35] and [36] for OFDM radar).
- *Detect and avoid:* When detecting interference in the measurement signal, the radar actively changes its signal to steer clear of interference in the subsequent cycles [37].
- *Interference-aware cognitive radar* [7]: The radar senses the entire operational spectrum and adaptively avoids interference via waveform adaptation [Figure 7(a)].
- *Centralized coordination* [8]: Self-driving cars are centrally coordinated to avoid radar interference [Figure 7(b)].

As these approaches range from local interference suppression at the receiver to coordinated interference avoidance, they widely vary in their sovereignty and universality. The latter class of methods requires other radars to conform to rules or cooperate, i.e., relies on actions of other radars. Methods from the first category are capable of suppressing interference of a specific form, and thus are effective only for certain interferers.

The methods based on suppression of interference at the receiver seek a representation where the interference and signal energy are maximally separable, such that the major portion of interference can be dropped without considerable loss of the radar signal. An example of such processing is mitigation of narrowband interference from OFDM radar by dropping the corrupted subcarriers [35]. Equivalently, for FMCW (fast-chirp) radar, interference from other FMCW sensors with different slopes can be filtered out from the time signal, since only a portion of the time signal is affected due to the antialiasing filter. The discarded portion of the radar signal needs to be recovered to prevent notable performance degradation. For signal recovery, methods ranging from linear prediction [35] to sparse recovery [33] may be used. Similarly, digital beamforming can be used to focus interference in the angular domain toward the DOA of the interferer, thus reducing it in all other directions [34]. Alternative approaches are based on estimating the interfering signal and its subsequent subtraction (e.g., [36]). Such methods heavily rely on known characteristics of the interfering signal. These methods for interference suppression have the drawback of being specific to a certain interference type. Furthermore, since in practice perfect separation of signal from interference is often impossible, such approaches discard a portion of the radar signal. Moreover, they do not improve the overall interference situation, but only suppress it locally at the receiver, and thus typically serve as the last resort for interference mitigation.

Intuitively, a more preferable approach is interference avoidance instead of postprocessing. This requires active adaptation of the Tx signal. An approach inspired by the interference-avoidance mechanism of bats is to gradually steer clear after detecting interference in the received signal by adjusting the carrier frequency [37]. This avoids interference instead of its local suppression, and thus benefits both parties. It also does not require cooperation from the interferer. This method approaches its limits when the density of interferers makes it impractical to blindly move in frequency at a risk of interfering with another, initially unknown radar signal operating at a different frequency.

A more universal solution for adaptive interference avoidance is interference-aware cognitive radar (IACR) [7], which adopts the principles of cognitive radar [38], [39] to remedy the automotive interference problem. IACR comprises the following three main blocks [Figure 7(a)]:

- *Spectrum sensing*: This continuously analyzes the operational spectral band for interference and delivers the spectral occupancy information.
- *Spectrum interpretation*: This contains the cognitive intelligence of the system. It is responsible for applying reasoning to the information obtained via spectrum sensing by means of detection and classification of interfering signals. It also estimates various interference parameters. Based on this knowledge, prediction of the interference behavior for the next transmission cycle is performed. This serves as a basis for choosing an optimal adaptation strategy for the next measurement cycle.
- *Waveform adaptation*: This comprises possible adaptation methods along with the corresponding signal processing algorithms. It also sets in motion the chosen adaptation strategy. The goal is to avoid interference dynamically, while maintaining the radar estimation performance. Possible adaptation space is frequency, time, and waveform.

An implementation of IACR in [7] uses a smaller portion of the operational bandwidth available for automotive radar (e.g., 0.5 GHz in the frequency range 77–81 GHz) and avoids interference by adaptation of the carrier frequency and starting time of the measurement. Based on spectrum sensing and interpretation, the carrier frequency is adapted for each measurement cycle within the entire available bandwidth to maximally mitigate interference from other radar sensors. Depending on the chosen strategy, this may imply not only cycle-to-cycle hopping of the carrier frequency, but also gradual adaptation within the measurement cycle itself. By adaptively avoiding interference from other automotive radars, IACR obtains robustness against interference in a universal, interference-agnostic manner and already in the analog domain, i.e., by avoidance instead of post-treatment. This mitigates the overall interference problem through cognitive interference avoidance, benefitting the currently deployed, nonintelligent and nonadaptive systems through cognitive interference avoidance. Thus, it represents a promising path for automotive radar to improve the interference situation. An open issue is, however, interference avoidance between multiple IACRs operating in the same environment, as each acting autonomously could potentially lead to mutual interference. To this end, sets of rules or well-defined mechanisms are needed to ensure predictable behavior.

A conceptually different approach for automotive interference mitigation is the RadarMAC architecture for centralized coordination of radar sensors on self-driving cars (Figure 7(b)). This approach requires vehicles to communicate their locations and routes to a control center, which represents the radar operation schedule of vehicles in the same environment as a graph coloring problem and determines playbooks for each self-driving car for their radars to operate interference-free. Especially suited for dense interference settings, centralized coordination is a promising approach for reducing overall interference. It requires, however, an additional reliable communication link, availability at all times, and participants obeying a central coordinator. Thus, it does not address the problem of interference with existing nonadaptive, noncooperative radar sensors operating at the same frequency band.

Conclusions

As automated driving technology evolves, automotive radar is taking major steps toward becoming a more powerful environment sensor. This transformation involves all aspects of automotive radar, including system concept, modulation, and signal processing. In this article we summarized the major trends in the field of automotive radar especially relevant for high-performance radar systems designed for self-driving cars. One primary development is radar operating with arbitrary digitally generated waveforms. Multicarrier modulations, such as OFDM, not only enable radar and communication to be combined in a single waveform, but also represent means for implementing new software-defined radar concepts. In the context of MIMO radar, multicarrier modulations permit the generation of a wide variety of orthogonal waveforms, enabling advantageous multiplexing schemes.

Based on a generalized signal model, we described the simplifications behind the conventional radar signal processing that no longer hold when upscaling radar parameters to increase performance. We reviewed a signal processing framework based on more rigorous modeling of radar signals that allows migration-free and Doppler-robust performance at a moderate computational cost. Finally, we surveyed automotive radar interference-mitigation methods. As automotive radar technology penetrates the market, the interference problem becomes more acute, which means that methods for suppressing interference locally at the receiver will not be sufficient. Promising paradigms for interference mitigation in adaptive, cognitive, and/or coordinated manner arise, and their role in improving the overall interference situation is becoming increasingly apparent. Although automotive radar has been known for decades, this review indicates that there is a fertile ground for research, stimulated by the development of self-driving cars.

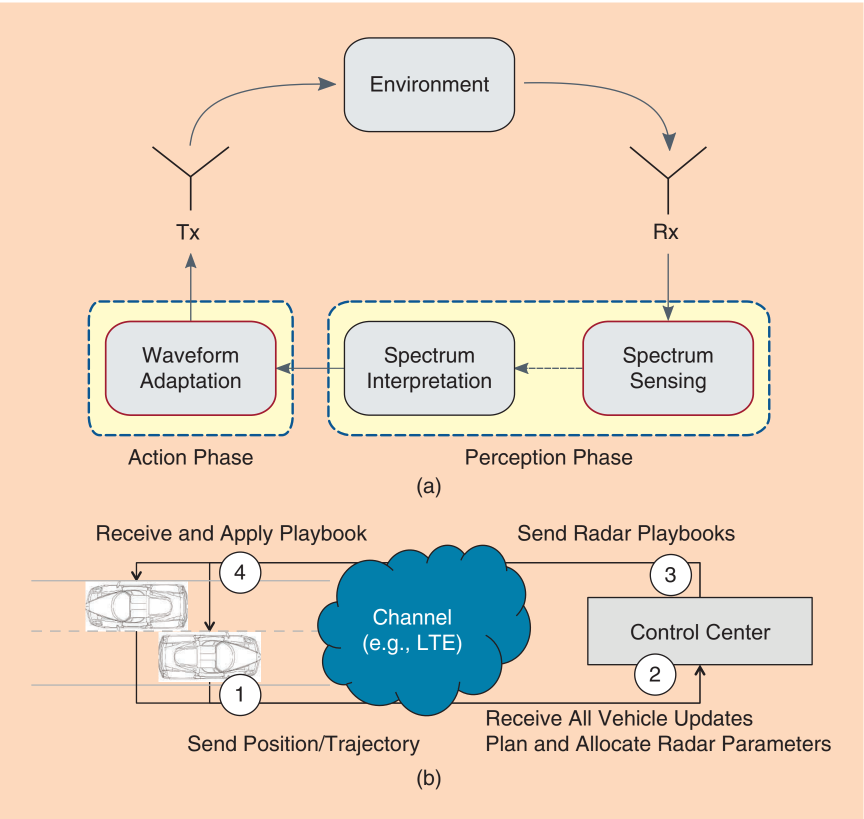

FIGURE 7. Diagram and illustration showing new paradigms for adaptive interference mitigation. (a) Closed-loop perception–action cycle of interference-aware cognitive radar [7]. (b) System overview of RadarMAC architecture for coordinated interference avoidance [8].

Authors

Gor Hakobyan (Gor.Hakobyan@de.bosch.com) received his B.E. and M.E. degrees in radio and communication engineering from the National Polytechnic University of Armenia in 2011 and 2013, respectively, and his Dr.-Ing. degree in electrical engineering from the University of Stuttgart, Germany, in 2018. He received the Best Paper Award in the Young Scientist Contest at the 2016 International Radar Symposium. He joined the Corporate Research Division of Robert Bosch GmbH and is now a research scientist in the field of radar signal processing and system design. His current research interests include radar signal processing, compressed sensing, radar modulation schemes, and interference-mitigation techniques.

Bin Yang (Bin.Yang@iss.uni-stuttgart.de) received his Dipl.-Ing. and Ph.D. degrees in electrical engineering in 1986 and 1991, respectively, from the Ruhr University Bochum. He is a professor and the head of the Institute for Signal Processing and System Theory in the Faculty of Computer Science, Electrical Engineering and Information Technology at the University of Stuttgart, Germany. His research interests include algorithms and applications of signal processing and machine learning, in particular radar signal processing, energy monitoring, and medical signal processing, with an increasing focus on deep-learning methods.

References

[1] D. M. Grimes and T. O. Jones, "Automotive radar: A brief review," in *Proc. IEEE*, vol. 62, no. 6, pp. 804–822, June 1974.

[2] E. Guizzo, "How Google's self-driving car works," *IEEE Spectrum*, Oct. 11, 2011. [Online]. Available: https://spectrum.ieee.org/automaton/robotics/artificial-intelligence/how-google-self-driving-car-works

[3] H. H. Meinel, "Evolving automotive radar—from the very beginnings into the future," in *Proc. 8th European Conf. Antennas and Propagation (EuCAP 2014)*, Apr. 2014, pp. 3107–3114.

[4] F. Foelster and H. Rohling, "Signal processing structure for automotive radar," *Frequenz*, vol. 60, no. 1–2, 2006. doi: 10.1515/FREQ.2006.60.1-2.20.

[5] J. Hasch, E. Topak, R. Schnabel, T. Zwick, R. Weigel, and C. Waldschmidt, "Millimeter-wave technology for automotive radar sensors in the 77 GHz frequency band," *IEEE Trans. Microw. Theory Techn.*, vol. 60, no. 3, pp. 845–860, Mar. 2012.

[6] S. M. Patole, M. Torlak, D. Wang, and M. Ali, "Automotive radars: A review of signal processing techniques," *IEEE Signal Process. Mag.*, vol. 34, no. 2, pp. 22–35, Mar. 2017.

[7] G. Hakobyan, "Orthogonal frequency division multiplexing multiple-input multiple-output automotive radar with novel signal processing algorithms," Ph.D. dissertation, Univ. of Stuttgart, Germany, 2018. [Online]. Available: http://dx.doi.org/10.18419/opus-9830

[8] J. Khoury, R. Ramanathan, D. McCloskey, R. Smith, and T. Campbell, "Radarmac: Mitigating radar interference in self-driving cars," in *Proc. 2016 13th Annu. IEEE Int. Conf. Sensing, Communication, and Networking (SECON)*, June 2016. doi: 10.1109/SAHCN.2016.7733011.

[9] M. Kronauge and H. Rohling, "New chirp sequence radar waveform," *IEEE Trans. Aerosp. Electron. Syst.*, vol. 50, no. 4, pp. 2870–2877, Oct. 2014.

[10] H. Rohling, "Radar CFAR thresholding in clutter and multiple target situations," *IEEE Trans. Aerosp. Electron. Syst.*, vol. AES-19, no. 4, pp. 608–621, July 1983.

[11] L. Hammarstrand, L. Svensson, F. Sandblom, and J. Sorstedt, "Extended object tracking using a radar resolution model," *IEEE Trans. Aerosp. Electron. Syst.*, vol. 48, no. 3, pp. 2371–2386, July 2012.

[12] S. A. Askeland and T. Ekman, "Tracking with a high-resolution 2D spectral estimation based automotive radar," *IEEE Trans. Intell. Transp. Syst.*, vol. 16, no. 5, pp. 2418–2423, Oct. 2015.

[13] Z. Ji, M. Luciw, J. Weng, and S. Zeng, "Incremental online object learning in a vehicular radar-vision fusion framework," *IEEE Trans. Intell. Transp. Syst.*, vol. 12, no. 2, pp. 402–411, June 2011.

[14] H. Krim and M. Viberg, "Two decades of array signal processing research: The parametric approach," *IEEE Signal Process. Mag.*, vol. 13, no. 4, pp. 67–94, July 1996.

[15] F. Engels, P. Heidenreich, A. M. Zoubir, F. K. Jondral, and M. Wintermantel, "Advances in automotive radar: A framework on computationally efficient high-resolution frequency estimation," *IEEE Signal Process. Mag.*, vol. 34, no. 2, pp. 36–46, Mar. 2017.

[16] D. Cohen and Y. C. Eldar, "Sub-Nyquist radar systems: Temporal, spectral, and spatial compression," *IEEE Signal Process. Mag.*, vol. 35, no. 6, pp. 35–58, Nov. 2018.

[17] C. Sturm and W. Wiesbeck, "Waveform design and signal processing aspects for fusion of wireless communications and radar sensing," in *Proc. IEEE*, July 2011, vol. 99, pp. 1236–1259.

[18] A. Bourdoux, U. Ahmad, D. Guermandi, S. Brebels, A. Dewilde, and W. V. Thillo, "PMCW waveform and MIMO technique for a 79 GHz CMOS automotive radar," in *Proc. 2016 IEEE Radar Conf. (RadarConf)*, May 2016. doi: 10.1109/RADAR.2016.7485114.

[19] X.-g. Xia, T. Zhang, and L. Kong, "MIMO OFDM radar IRCI free range reconstruction with sufficient cyclic prefix," *IEEE Trans. Aerosp. Electron. Syst.*, vol. 51, no. 3, pp. 2276–2293, July 2015.

[20] B. Schweizer, C. Knill, D. Schindler, and C. Waldschmidt, "Stepped-carrier OFDM-radar processing scheme to retrieve high-resolution range-velocity profile at low sampling rate," *IEEE Trans. Microw. Theory Techn.*, vol. 66, no. 3, pp. 1610–1618, Mar. 2018.

[21] D. Schindler, B. Schweizer, C. Knill, J. Hasch, and C. Waldschmidt, "MIMO-OFDM radar using a linear frequency modulated carrier to reduce sampling requirements," *IEEE Trans. Microw. Theory Techn.*, vol. 66, no. 7, pp. 3511–3520, July 2018.

[22] C. Knill, B. Schweizer, S. Sparrer, F. Roos, R. F. H. Fischer, and C. Waldschmidt, "High range and Doppler resolution by application of compressed sensing using low baseband bandwidth OFDM radar," *IEEE Trans. Microw. Theory Techn.*, vol. 66, no. 7, pp. 3535–3546, July 2018.

[23] J. Li and P. Stoica, "MIMO radar with colocated antennas," *IEEE Signal Process. Mag.*, vol. 24, no. 5, pp. 106–114, Sept. 2007.

[24] A. Zwanetski and H. Rohling, "Continuous wave MIMO radar based on time division multiplexing," in *Proc. 2012 13th Int. Radar Symp.*, May 2012, pp. 119–121.

[25] C. Pfeffer, R. Feger, C. Wagner, and A. Stelzer, "FMCW MIMO radar system for frequency-division multiple TX-beamforming," *IEEE Trans. Microw. Theory Techn.*, vol. 61, no. 12, pp. 4262–4274, Dec. 2013.

[26] H. Haderer, R. Feger, C. Pfeffer, and A. Stelzer, "Millimeter-wave phase-coded CW MIMO radar using zero- and low-correlation-zone sequence sets," *IEEE Trans. Microw. Theory Techn.*, vol. 64, no. 12, pp. 4312–4323, Dec. 2016.

[27] G. Hakobyan and B. Yang, "A novel OFDM-MIMO radar with non-equidistant subcarrier interleaving and compressed sensing," in *Proc. 17th Int. Radar Symp. (IRS)*, 2016. doi: 10.1109/IRS.2016.7497312.

[28] G. Hakobyan and B. Yang, "A novel OFDM-MIMO radar with non-equidistant dynamic subcarrier interleaving," in *Proc. 2016 European Radar Conf. (EuRAD)*, Oct. 2016, pp. 45–48.

[29] R. P. Perry, R. C. DiPietro, and R. L. Fante, "Coherent integration with range migration using keystone formatting," in *Proc. 2007 IEEE Radar Conf.*, Apr. 2007, pp. 863–868.

[30] G. Hakobyan and B. Yang, "A novel intercarrier-interference free signal processing scheme for OFDM radar," *IEEE Trans. Veh. Technol.*, vol. 67, no. 6, pp. 5158–5167, June 2018.

[31] R. F. Tigrek and P. V. Genderen, "Compensation of range migration for cyclically repetitive Doppler-sensitive waveform (OFDM)," *IEEE Trans. Aerosp. Electron. Syst.*, vol. 46, no. 4, pp. 2118–2123, Oct. 2010.

[32] M. Kunert, "The EU project MOSARIM: A general overview of project objectives and conducted work," in *Proc. 2012 9th European Radar Conf.*, Oct. 2012, pp. 1–5.

[33] J. Bechter, F. Roos, M. Rahman, and C. Waldschmidt, "Automotive radar interference mitigation using a sparse sampling approach," in *Proc. 2017 European Radar Conf. (EURAD)*, Oct. 2017, pp. 90–93.

[34] J. Bechter, M. Rameez, and C. Waldschmidt, "Analytical and experimental investigations on mitigation of interference in a DBF MIMO radar," *IEEE Trans. Microw. Theory Techn.*, vol. 65, no. 5, pp. 1727–1734, May 2017.

[35] G. Hakobyan and B. Yang, "A novel narrowband interference suppression method for OFDM radar," in *Proc. 24th European Signal Processing Conf. (EUSIPCO)*, 2016. doi: 10.1109/EUSIPCO.2016.7760645.

[36] Y. L. Sit, B. Nuss, and T. Zwick, "On mutual interference cancellation in a MIMO OFDM multiuser radar-communication network," *IEEE Trans. Veh. Technol.*, vol. 67, no. 4, pp. 3339–3348, Apr. 2018.

[37] J. Bechter, C. Sippel, and C. Waldschmidt, "Bats-inspired frequency hopping for mitigation of interference between automotive radars," in *Proc. 2016 IEEE MTT-S Int. Conf. Microwaves for Intelligent Mobility (ICMIM)*, May 2016. doi: 10.1109/ICMIM.2016.7533928.

[38] S. Haykin, "Cognitive radar: A way of the future," *IEEE Signal Process. Mag.*, vol. 23, no. 1, pp. 30–40, Jan. 2006.

[39] M. S. Greco, F. Gini, P. Stinco, and K. Bell, "Cognitive radars: On the road to reality: Progress thus far and possibilities for the future," *IEEE Signal Process. Mag.*, vol. 35, no. 4, pp. 112–125, July 2018.

SP